COBEM2017-1496
EFFECTS OF INJECTION TIMING ON PERFORMANCE, COMBUSTION AND EMISSIONS OF A GASOLINE DI ENGINE

Vitor Vielmo Cogo
Macklini Dalla Nora
André Nakaema Aronis
Mario Eduardo dos Santos Martins
UFSM - Universidade Federal de Santa Maria, Grupo de pesquisa em motores,combustíveis e emissões (GPMOT)
vvcogo.14@gmail.com
mack@gepoc.ufsm.br
andrearonis@gmail.com
mario@mecanica.ufsm.br

Thompson Diordinis Metzka Lanzanova
Brunel University London, Centre for Advanced Powertrain and Fuels (CAPF), Kingston Ln, London, Uxbridge UB83PH, United Kingdon
lanzanova@gmail.com

Abstract. *With the purpose of achieving better fuel efficiency, gasoline direct injection (DI) has been highly implemented on spark ignition internal combustion engines (ICE). A great advantage of this fuel injection method compared to port fuel injection (PFI) is the higher charge cooling effect and better fuel atomization process as a result of increased fuel pressure, which may reduce knock tendency. In this work, the injection timing in a DI engine was varied within the intake stroke to investigate its effects on the combustion, gaseous emissions and performance of the engine. The trade-off between efficiency and emissions was sought by using a side-mounted multi-hole gasoline injector on a spark ignition (SI) engine. The fuel pressure was kept constant at 14.5±0.5 MPa and its temperature at 295±5 K. It was found that later injection timings during the intake stroke resulted in more pronounced charge cooling effect, thus providing lower in-cylinder temperatures and nitrogen oxides (NO_x) emissions. However, higher combustion duration could be observed due to combustion deterioration and more advanced spark timings were made necessary to maintain the optimum combustion phasing.*

Keywords: gasoline direct injection, homogeneous charging, spark ignition combustion

1. INTRODUCTION

Aiming at better fuel efficiency and lower carbon dioxide emissions (CO_2), gasoline direct injection has been widely implemented on spark ignition internal combustion engines (ICE)(Zhao et al., 1999). There are many advantages of direct injection (DI) compared to port fuel injection (PFI). In DI engines, fuel injection can occur at any time within the cycle, which has enabled, for instance, unthrottled operation by means of stratified combustion (Zhao, 2005). Homogeneous charging mode (HCM), is generally preferred when partial to high load is imposed and stoichiometric to slightly rich air-fuel mixture are needed (Kume et al., 1996). With optimized injection timing for HCM i.e., not so close to top dead center of intake stroke (TDC_i) or to bottom dead center of intake stroke (BDC_i), more pronounced charge cooling effect occurs. It results from more heat being absorbed from the combustion chamber for its vaporization instead of heat from the intake port and back of valve, therefore displacing less air and increasing the volumetric efficiency as well (Chincholkar and Suryawanshi, 2016). Combustion phasing is also improved due to lower charge temperature at the end of its compression.

With the fuel injection occurring during the compression stroke i.e., stratified charging mode (SCM), improved start-ability at cold start conditions is obtained (Banerjee and Kumar, 2016). This can be explained by the higher injected fuel pressure providing better fuel atomization at lower temperatures, which also reduces unburned hydrocarbons emissions (HC). SCM operation provides the possibility of operating with charge dilution and global lean air-fuel mixture reducing heat losses. This is possible if an ignitable air-fuel mixture is maintained around the spark plug, which enables higher overall efficiency due to lower pumping losses and lower specific heats ratio (γ)(Fansler et al., 2015). The disadvantages of SCM operation are the higher particulate matter emissions (PM) due to poor charge homogeneity and fuel impingement, as well as the inability of NOx emissions being reduced by conventional three way catalyst (TWC) (Whitaker et al., 2011).

In this work, the effects of injection timing represented by the start of injection (SOI) were studied. Engine operation was performed on HCM with start of injection (SOI) occurring only within the intake stroke. The goal of this study was to evaluate the trade-off between efficiency and emissions of the engine operating with gasoline RON 95.

2. EXPERIMENTAL PROCEDURE

A single cylinder four-stroke Ricardo Hydra Camless engine coupled to an active dynamometer was employed, with a displaced volume of 350 cm^3, geometric compression ratio of 11.8:1 and a four-valve pent-roof combustion chamber (Lanzanova et al., 2016). The fully flexible electro-hydraulic valve system enabled infinite variation on intake and exhaust valve timings and lifts. Engine coolant and oil temperature was kept at 353 ± 2 K, while the fuel was kept at a constant injection pressure of 14.5± 0.5 MPa and temperature of 295± 5 K. The injection timing was varied within the intake stroke at the constant engine load of 0.6± 0.01 MPa indicated mean effective pressure (IMEP) and 1500 rpm. Stoichiometric air-fuel ratio was maintained during all test points. A side-mounted multi-hole gasoline injector was used, and fuel flow rate was measured with a Coriolis mass flow meter. Figure 1(a) depicts the experimental setup.The minimum spark advance for best torque was obtained so the combustion phasing i.e., 50% of the burned mass were maintained around 10 CAD after Top Dead Center fire (TDC$_f$)(Heywood, 1988). A conventional valve timing was chosen for this study operating with a short positive valve overlap (PVO). This is presented in figure 1(b) with the tested SOI. Where TCD$_i$ and BDC$_i$ are represented as 360 and 540 crank angle degree (CAD) respectively. Tailpipe emissions were measured with a Horiba MEXA 7170DEGR and converted from parts per million (ppm) to g/kWh by means of UN regulation number 49 (Nations, 2013). The measurement uncertainty analysis was performed following the propagation of uncertainty theory (Taylor, 1997).
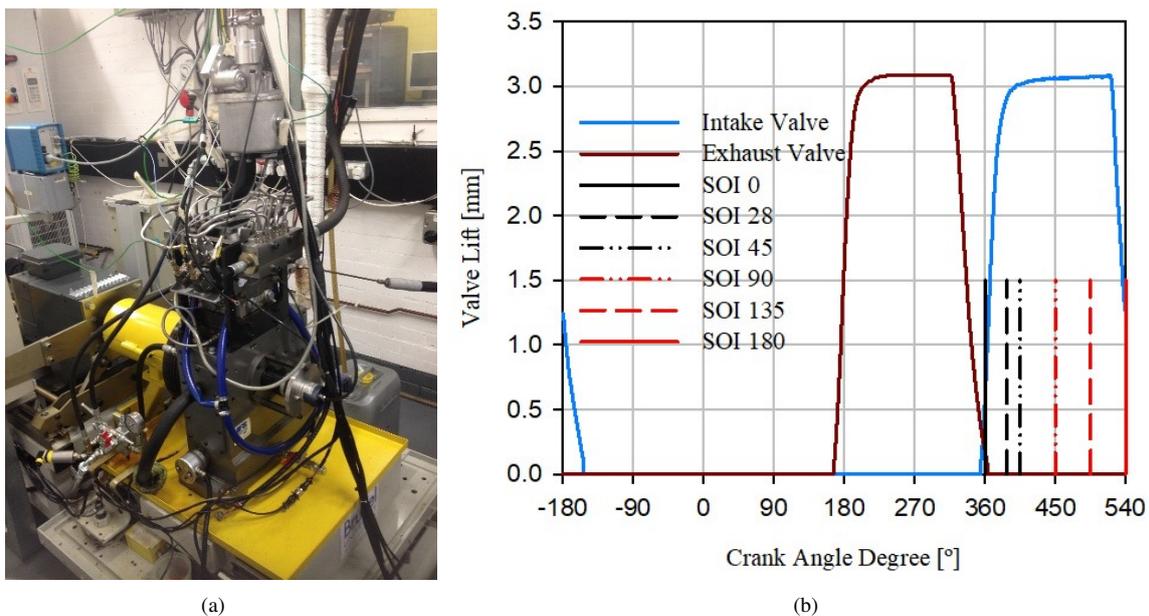

Figure 1. (a): Ricardo Hydra Camless engine (b): Valve timing and SOI

The combustion analysis was performed with the acquired in-cylinder pressure data by calculating the apparent heat release rate (AHRR) from zero-dimensional models (Abbaszadehmosayebi and Ganippa, 2014) (Canakci et al., 2009). AHRR was obtained from in-cylinder pressure data and crankshaft position. To use this model a ratio of specific heats must be specified, in this manner, the averaged polythropic expoent throughout a well-defined section of the compression and expansion strokes were obtained (Alagumalai, 2015). Then the AHRR was integrated and normalized to obtain the mass fraction burned (MFB). In-cylinder temperature can be represented with a ideal gas model where temperature, pressure and volume change within the cycle and mass and gas constant (R) remain constant. The thermodynamics properties of the working fluid throughout the cycle are compared with those at the intake valve closure (IVC) so the instantaneously in-cylinder temperature could be estimated. The air excess ratio (λ) was estimated from engine-out emissions data (Silvis, 1997). The flame development angle was obtained by the difference between the spark time and the 10% of MFB while the combustion duration was the difference between the 10% and 90% of MFB. The combustion efficiency is a measure to define how much of the fuel was converted to useful heat. Where 100% of combustion efficiency means the combustion process has generated only CO$_2$ and H$_2$O vapour as products. The indicated efficiency was obtained by the comparison of the indicated power produced by the engine with the fuel mass flow rate and the lower heating value of the fuel (LHV_f).

3. RESULTS AND DISCUSSION

The results of this study were divided into three subsection as follows. The combustion subsection treated about the shape of the heat release rate trace and its implications on the engine operation. The emissions subsection evaluated the engine-out emissions and its causes. And finally, the performance subsection gathered all data into an overall result. The results are presented by the start of injection in crank angle degree after Top Dead Center of intake stroke (CAD ATDCi).
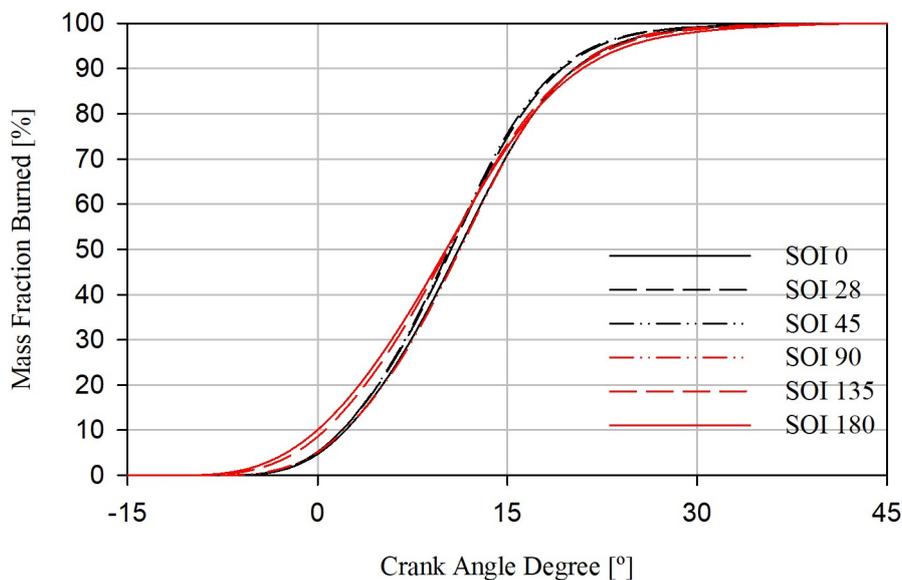
3.1 Combustion

The combustion parameters were evaluated through the AHRR. The AHRR and MFB are shown in figures 2(a) and 2(b) respectively for all SOI points. In-cylinder temperature is shown in figure 2(c). As the injection timings were retarded combustion deteriorated and weaker heat release rate could be noticed mainly for SOI 180 $^\circ$ and SOI 135 $^\circ$.
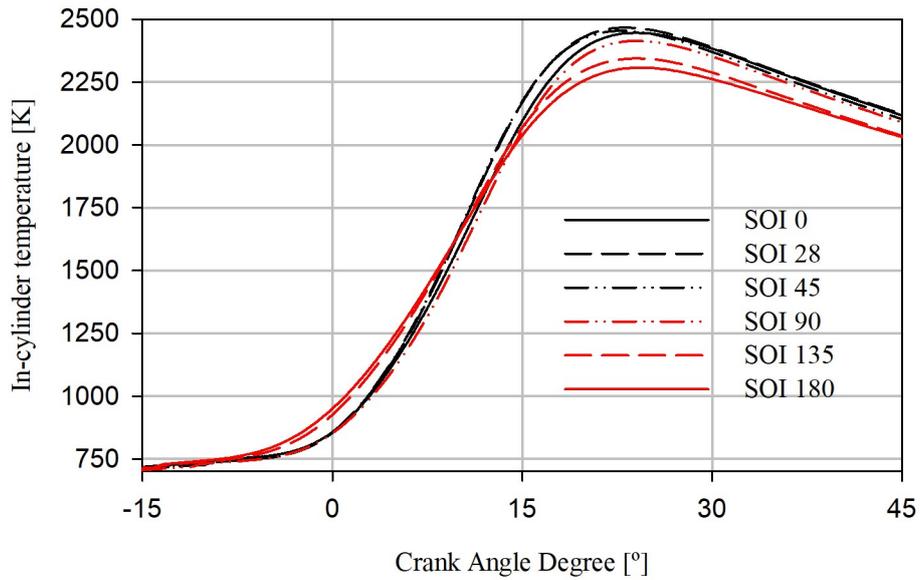
As the SOI reached an optimum point for the combustion event at about 45 $^\circ$, the AHRR decreased again towards SOI 180. In this condition the later injection timings compromised the charge homogeneity and more advanced spark timings were required. Lower in-cylinder temperatures were also obtained as observed in figure 2(c).
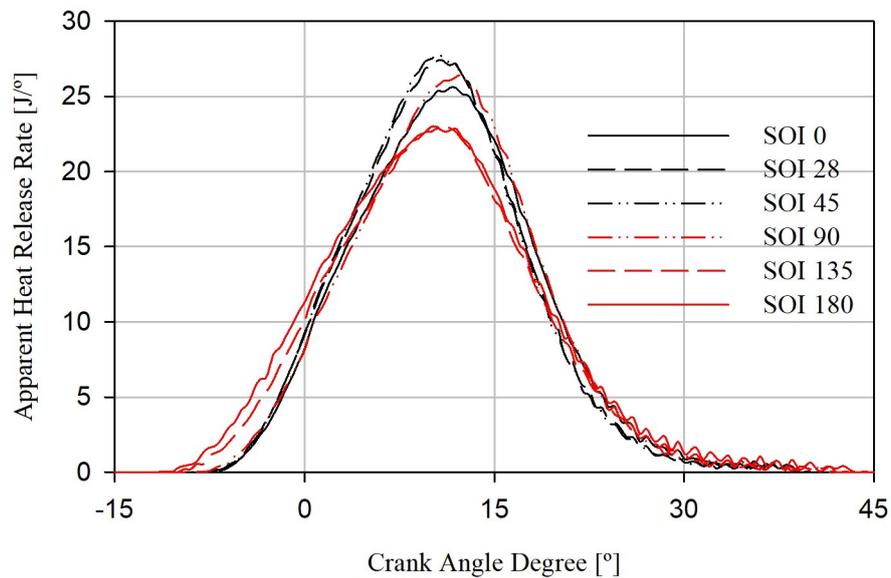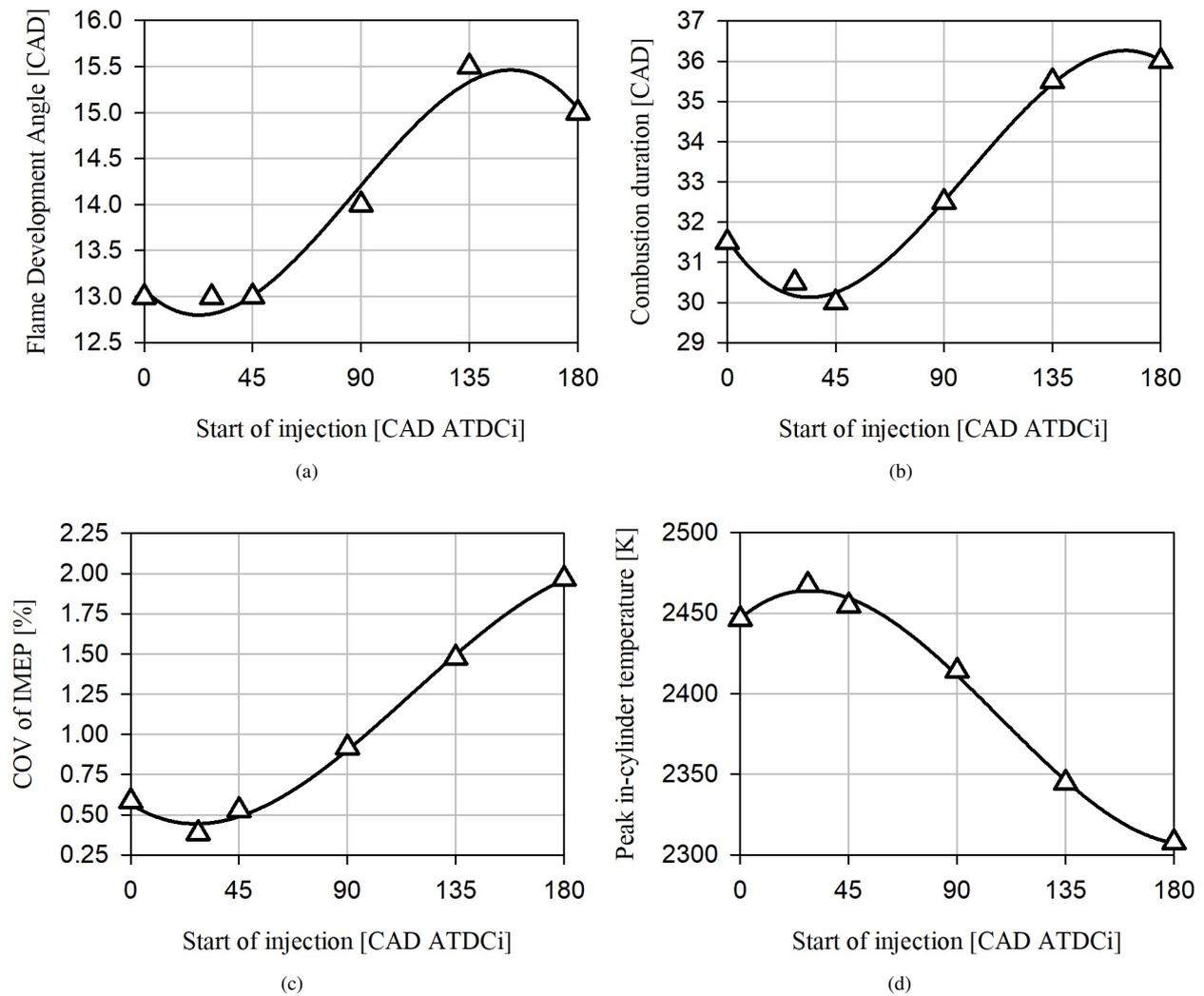

(a)

(b)

(c)

Figure 2. (a): Heat Release Rate (b): Mass Fraction Burned (c): In-cylinder temperature

(a)

(b)

(c)

(d)

Figure 3. (a): Flame Development Angle (b): Combustion duration (c): COV of IMEP (d): Peak in-cylinder temperature

At SOI 0, a lower peak of heat release rate and slower MFB also occurred explained by a characteristic fuel impinge-ment onto the piston wall which normally occurs due to the proximity of the piston and injector on this angular position for the studied engine. Therefore forming a fuel film on the piston surface and making it harder to vaporize and burn.

Figure 3(a) and 3(b) express that for later injection timings combustion deteriorated due to poor air-fuel mixing, either by fuel impingement for SOI lower than 45 º or by insufficient time available for the charge preparation at SOI higher than 45 º. Cyclic variability was measured by the coefficient of variation of IMEP (COV of IMEP) and is presented at figure 3(c). COV of IMEP has also increased for later injection timing which may occurred due to poorer mixture preparation which is directly linked to combustion instability. Following this trend the poorer combustion at later SOI could be confirmed by lower peak in-cylinder temperatures, displayed at figure 3(d).

3.2 Emissions

Indicated specific CO emissions (ISCO) is shown in figure 4(a). As it was expected higher CO emissions occurred for the later injection timings. The main cause of this increase may be the lower available time for mixture preparation leading to a non-homogeneous mixture, hence rich regions were created within the cylinder and complete CO oxidation into CO_2 became difficult (Ferguson and Kirkpatrick, 2001). Higher CO emissions at earliest point tested was probably justified by pool flames formed on the piston top due to fuel impingement.
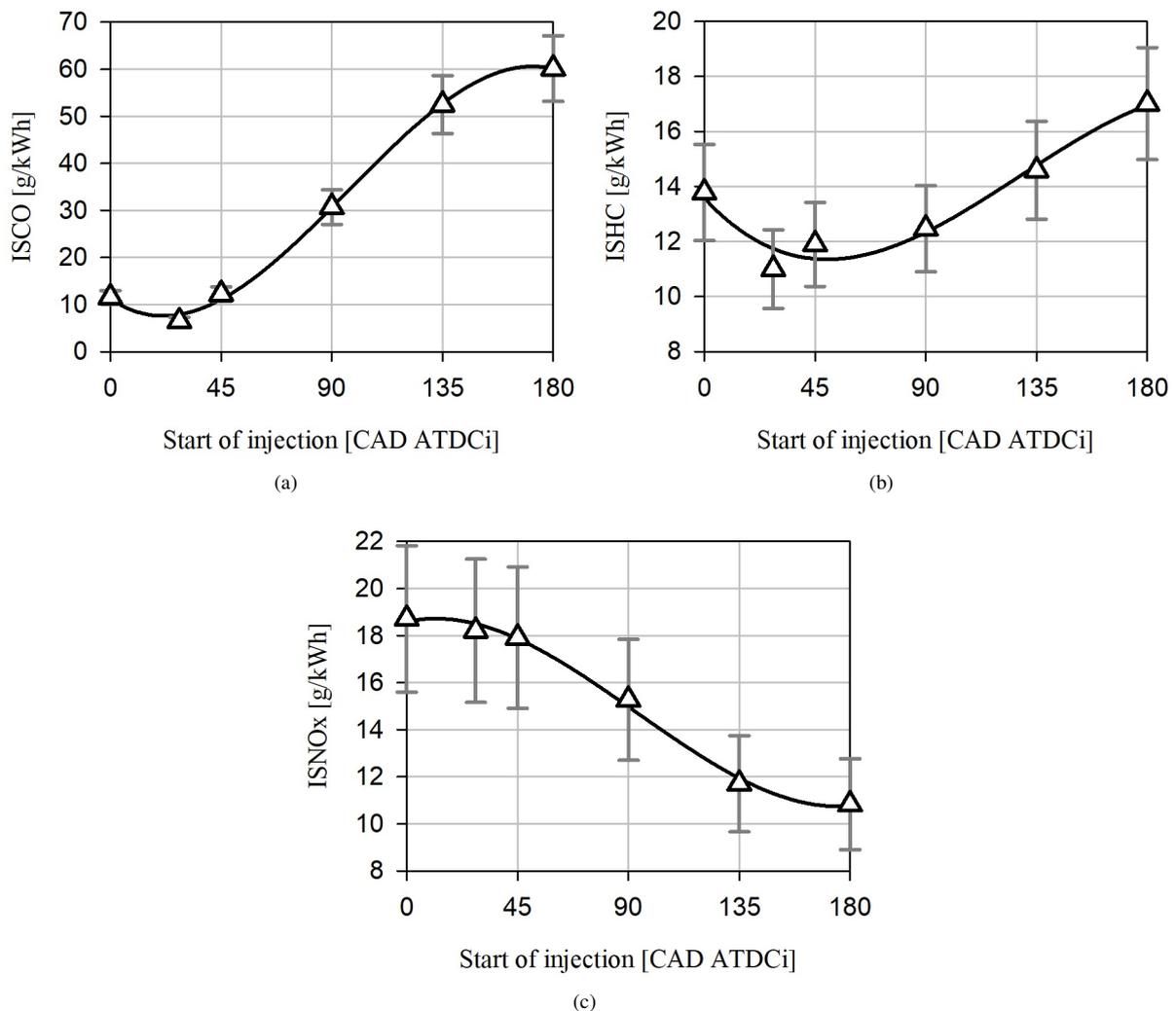

(a)

(b)

(c)

Figure 4. (a): Indicated specific CO emissions (b): Indicated specific NOx emissions (c): Indicated specific HC emissions

Indicated specific HC emissions (ISHC) are reported on figure 4(b). As it can be inferred at point SOI 0, higher ISHC emissions occurred compared to the intermediate points (SOI 28, 45 and 90). This occurrence also occurred from the fuel impingement which have made fuel vaporization harder. The greater values of ISHC for later injection timings could be justified by fuel impingement on the cylinder liner, as the in-cylinder pressure was lower in those conditions (weaker droplet aerodynamic breakup) and the fuel spray penetration reached farther. Another explanation for the higher HC

emissions at these points is the higher charge cooling effect which lowered charge temperature and helped the combustion deterioration.

Indicated specific NO_x emissions ($ISNO_x$) are shown in figure 4(c) directly linked to in-cylinder temperatures on figure 2(c) and 3(d). On the earlier injection timings (SOI 0, 28 and 45) combustion occurred successfully confirmed by higher in-cylinder temperatures (Stone, 1992). Lower charge cooling effect compared to later injection timings may have taken on these conditions also allowing higher charge temperature. Following this trend the later injection timings (SOI 135 and 180) showed higher charge cooling effect. Therefore lower heat release was expected due to lower initial charge temperature. Also figure 3(c) has shown the increased cyclic variability which is directly related to the explained combustion deterioration at the later injection points.

3.3 Performance

As a summary of all results presented until this subsection the performance subsection is presented. Figure 5(a) presents the combustion efficiency. As it could be expected the combustion efficiency followed the trend of ISCO, ISHC and peak in-cylinder temperature presented on figures 4(a), 4(b) and 3(d), respectively. This trend shows that for later injection timings the mixture formation has deteriorated and led to higher CO and HC emissions and lower released heat.

Figure 5(b) shows the indicated efficiency for all tested points. The only variable on this case is the fuel consumption as the engine operation condition and the fuel are the same for all testing points. Lower values of indicated efficiency were found at the later injection points. The main plausible reason is the high combustion inefficiency at these points which required more injected fuel mass to maintain the same load.

Both combustion and indicated efficiency are directly linked to high peak in-cylinder temperatures, low CO and HC emissions and fast combustion which as presented on figures 3(d), 4(a) ,4(b) and 2(b) ,respectively. The presented results showed plausible correlation with the presented theory.
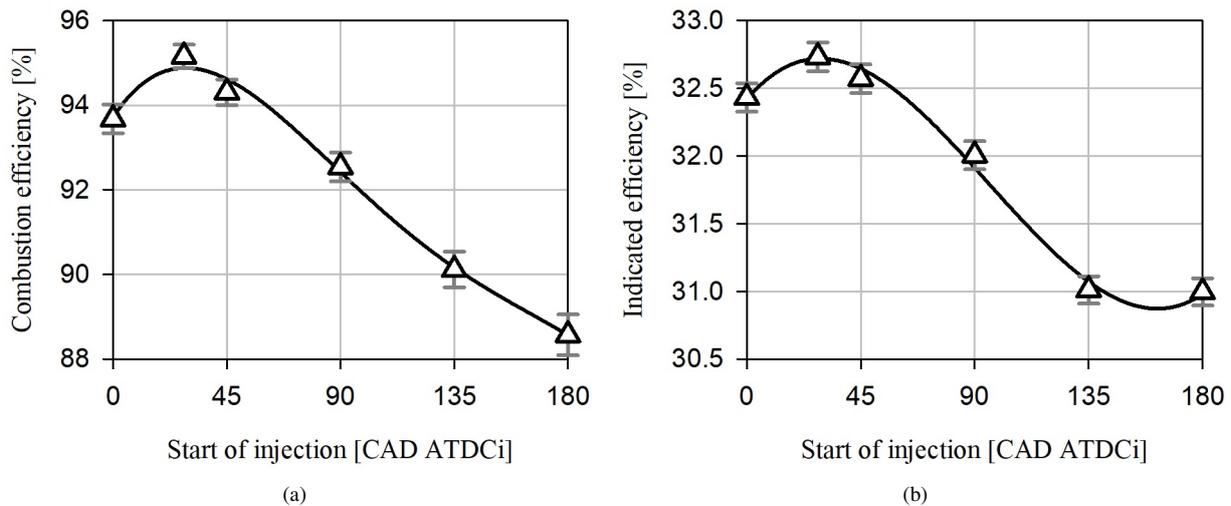

Figure 5. (a): Combustion Efficiency (b): Indicated Efficiency

Despite the high engine compression ratio (11.8:1), the relatively low overall values of indicated efficiency compared to conventional gasoline engines results from heat transfer due to the higher bore-to-stroke ratio of 1.2. For better fuel economy contemporary gasoline engines usually employ bore-to-stroke ratios in the range of 0.8 to 0.9.

4. CONCLUSIONS

The presented study evaluated the effects of injection timing on operational parameters of a gasoline direct injection engine. The main purpose of the study was to find a reasonable trade-off between performance and emissions on these engine operation points.

Even with lower ISNOx emissions the disadvantages of later injection timings were more prominent. Lower combustion efficiency and hence higher ISCO and ISHC emissions are very noticeable. A representative trade-off point may be the SOI 28 where the combustion and indicated efficiency are the highest found in the study followed by the lowest ISCO and ISHC. Comparing to the later injection point (SOI 180) a reduction of 89.2% occurred for ISCO and 35.4% for ISHC. On the other hand, an increase of 68.0% occurred for ISNOx as it was already expected due to better combustion conditions. This operating point represented very stable operating conditions with the lowest presented cyclic variability and fastest combustion.

5. REFERENCES

Abbaszadehmosayebi, G. and Ganippa, L. (2014). Determination of specific heat ratio and error analysis for engine heat release calculations. *Applied Energy*, 122:143–150.

Alagumalai, A. (2015). Combustion characteristics of lemongrass (Cymbopogon flexuosus) oil in a partial premixed charge compression ignition engine. *Alexandria Engineering Journal*, 54(3):405–413.

Banerjee, R. and Kumar, S. (2016). Numerical investigation of stratified air/fuel preparation in a GDI engine. *Applied Thermal Engineering*, 104:414–428.

Canakci, M., Ozsezen, A. N., and Turkcan, A. (2009). Combustion analysis of preheated crude sunflower oil in an IDI diesel engine. *Biomass and Bioenergy*, 33(5):760–767.

Chincholkar, S. and Suryawanshi, J. (2016). Gasoline Direct Injection: An Efficient Technology. *Energy Procedia*, 90:666–672.

Fansler, T. D., Reuss, D. L., Sick, V., and Dahms, R. N. (2015). Invited Review: Combustion instability in spray-guided stratified-charge engines: A review. *International Journal of Engine Research*, 16(3):260–305.

Ferguson, C. R. and Kirkpatrick, A. T. (2001). *Internal Combustion Engines: Applied Thermosciences*. 2nd edition.

Heywood, J. (1988). *Internal Combustion Engine Fundamentals*. McGraw-Hill, New York, 1 edition.

Kume, T., Iwamoto, Y., Iida, K., Murakami, M., Akishino, K., and Ando, H. (1996). Combustion control technologies for direct injection SI engine. Technical report, SAE technical paper.

Lanzanova, T. D. M., Dalla Nora, M., and Zhao, H. (2016). Performance and economic analysis of a direct injection spark ignition engine fueled with wet ethanol. *Applied Energy*, 169:230–239.

Nations, U. (2013). *Regulation No. 49: Uniform provisions concerning the measures to be taken against the emission of gaseous and particulate pollutants from compression-ignition engines and positive ignition engines for use in vehicles.*

Silvis, W. M. (1997). An algorithm for calculating the air/fuel ratio from exhaust emissions. Technical report, SAE Technical Paper.

Stone, R. (1992). *Introduction to Internal Combustion Engines*. 2nd edition.

Taylor, J. R. (1997). *An introduction to error analysis: The study of uncertainties in physical measurements*. University Science Books, Sausalito, California, 2nd edition.

Whitaker, P., Kapus, P., Ogris, M., and Hollerer, P. (2011). Measures to Reduce Particulate Emissions from Gasoline DI engines. *SAE International Journal of Engines*, 4(1):1498–1512.

Zhao, F., Lai, M.-C., and Harrington, D. L. (1999). Automotive spark-ignited direct-injection gasoline engines. *Progress in energy and combustion science*, 25(5):437–562.

Zhao, H. (2005). *Advanced direct injection combustion engine technologies and development: Gasoline and gas engines*, volume 1 of *Woodhead Publishing in materials*. Woodhead [u.a.], Cambridge, England. OCLC: 254469872.

6. RESPONSIBILITY NOTICE

The authors are the only responsible for the printed material included in this paper.